Electrical and magnetic properties of $(SrMnO_3)_n/(LaMnO_3)_{2n}$ superlattices

C. Adamo,[1] X. Ke,[2] P. Schiffer,[2] A. Soukiassian,[1] M. Warusawithana,[1] L. Maritato,[3] and D. G. Schlom[1,a)]

[1]*Department of Materials Science and Engineering, The Pennsylvania State University, University Park, Pennsylvania 16802-5005, USA*
[2]*Department of Physics, The Pennsylvania State University, University Park, Pennsylvania 16802, USA*
[3]*Dipartimento di Matematica ed Informatica, Università di Salerno, and CNR-INFM Coherentia Salerno, 84081, Baronissi (SA), Italy*

We report the magnetic and transport properties of $[(SrMnO_3)_n/(LaMnO_3)_{2n}]_m$ superlattices grown by molecular-beam epitaxy on (100) SrTiO$_3$ with periodicities n=1, 2, 3, 4, 5, 6, 8, and 16. Although the superlattice constituents, LaMnO$_3$ and SrMnO$_3$, are both antiferromagnetic insulators, for small n ($n \leqslant 2$) the superlattices behave like the ferromagnetic conductor La$_{0.67}$Sr$_{0.33}$MnO$_3$. As n increases, the magnetic properties become dominated by the LaMnO$_3$ layers, but the electronic transport properties continue to be controlled by the interfaces. © *2008 American Institute of Physics*. [DOI: 10.1063/1.2842421]

Interfaces, particularly between oxides with their full spectrum of electronic and magnetic properties, are an active area of research. Due to the structural and chemical compatibility of the perovskite-based transition metal oxides, high quality perovskite heterostructures can be realized, resulting in a variety of interesting and unexpected electronic and magnetic phenomena.[1–11] For instance, by controlling the termination layer at the LaAlO$_3$ and SrTiO$_3$ interface, where both LaAlO$_3$ and SrTiO$_3$ are nonmagnetic insulators, a magnetic[10] or superconducting[11] electron gas can be created.

Equally fascinating phenomena occur at the interfaces between magnetic oxides.[1–4,6–8,12–14] Recently, there are reports on the existence of ferromagnetism in $[(SrMnO_3)_n/(LaMnO_3)_{2n}]_m$ superlattices,[1,4,8,12–14] where both SrMnO$_3$ and LaMnO$_3$ are antiferromagnetic with Néel temperatures of 260 and 140 K, respectively.[15,16] The magnetization first increases with n, where n denotes the number of pseudocubic unit cells comprising the thickness of the SrMnO$_3$ layer of the heterostructure, and then decreases when n is larger than 4. This is attributed to the magnetic interaction and change transfer between Mn^{3+} and Mn^{4+} ions.[1,4]

Here, we report the magnetic properties of epitaxial $[(SrMnO_3)_n/(LaMnO_3)_{2n}]_m$ superlattices. For small n ($n \leqslant 2$), the superlattices behave like metallic, ferromagnetic La$_{0.67}$Sr$_{0.33}$MnO$_3$. With increasing n, the saturation magnetization and transition temperature decreases and the superlattices become more insulating (although still much more conductive than the constituent materials). We attribute the induced large magnetization and the high conductivity of the superlattices to charge transfer at the SrMnO$_3$/LaMnO$_3$ interface over a distance of a couple of unit cells.

We fabricated $[(SrMnO_3)_n/(LaMnO_3)_{2n}]_m$ superlattices with different values of n (n=1, 2, 3, 4, 5, 6, 8, and 16) and total film thickness of about 230 Å for $n \leqslant 6$ and about 200 Å for n=8 and 16. The superlattices were grown using shuttered layer-by-layer deposition[17] on buffered-HF treated (100)-SrTiO$_3$ substrates[18] in a reactive molecular-beam epitaxy (MBE) system equipped with reflection high-energy

electron diffraction. A substrate temperature of 700 °C and an oxidant (O$_2$+10% O$_3$) background partial pressure of 5 × 10^{-7} Torr, which was kept constant until the temperature of the substrate dropped below 200 °C, were used. The deposition of n layers of SrMnO$_3$ followed by $2n$ layers of LaMnO$_3$ yields a superlattice with an average stoichiometry of La$_{0.67}$Sr$_{0.33}$MnO$_3$. For comparison, SrMnO$_3$, LaMnO$_3$, and La$_{0.67}$Sr$_{0.33}$MnO$_3$ epitaxial thin films were also grown under the same conditions on (100) SrTiO$_3$. X-ray diffraction (XRD) θ-2θ scans and rocking curves were made on all superlattices to investigate their structural perfection. Electronic transport measurements were performed by standard four-probe measurements using a Quantum Design physical properties measuring systems. Magnetization measurements were carried out with a superconducting quantum interference device magnetometer (Quantum Design MPMS).

Figure 1 shows the out-of-plane XRD θ-2θ patterns of four $[(SrMnO_3)_n/(LaMnO_3)_{2n}]_m$ superlattices with n=1, 2, 3, and 4. The fundamental peaks and the satellite peaks due to A-site cation order are visible for all of the samples. The superlattice wavelengths were calculated to be 11.63 ± 0.09, 23.14 ± 0.57, 34.81 ± 0.49, and 46.2 ± 1.1 Å for the samples with n=1, 2, 3, and 4, respectively.[19] The rocking curve full width at half maximum (FWHM) of all of the $(SrMnO_3)_n/(LaMnO_3)_{2n}$ superlattices are less than 0.02°. These values are comparable to the rocking curve FWHM of the (100) SrTiO$_3$ substrates upon which they are grown.

The temperature dependence of the resistivity for different magnetic fields is shown in Figs. 2(a)–2(c) for n=2, 4, and 16. For $n \leqslant 2$, the superlattices show metallic behavior at low temperatures with smaller resistivities and higher transition temperatures at high magnetic fields [Fig. 2(a)], similar to the well know behavior of La$_{0.67}$Sr$_{0.33}$MnO$_3$ solid-solution samples.[20] The appearance of the maximum in the resistivity curves corresponds well to the onset of ferromagnetism.[12] The observed ferromagnetic metallic behavior in the $(SrMnO_3)_n/(LaMnO_3)_{2n}$ superlattices presumably results from the magnetic interaction between Mn^{3+} and Mn^{4+} at the interface between LaMnO$_3$ and SrMnO$_3$ layers. Doping divalent elements (Ca, Sr, and Ba) onto the La site introduces mixed valence Mn ions, leading to different magnetic and
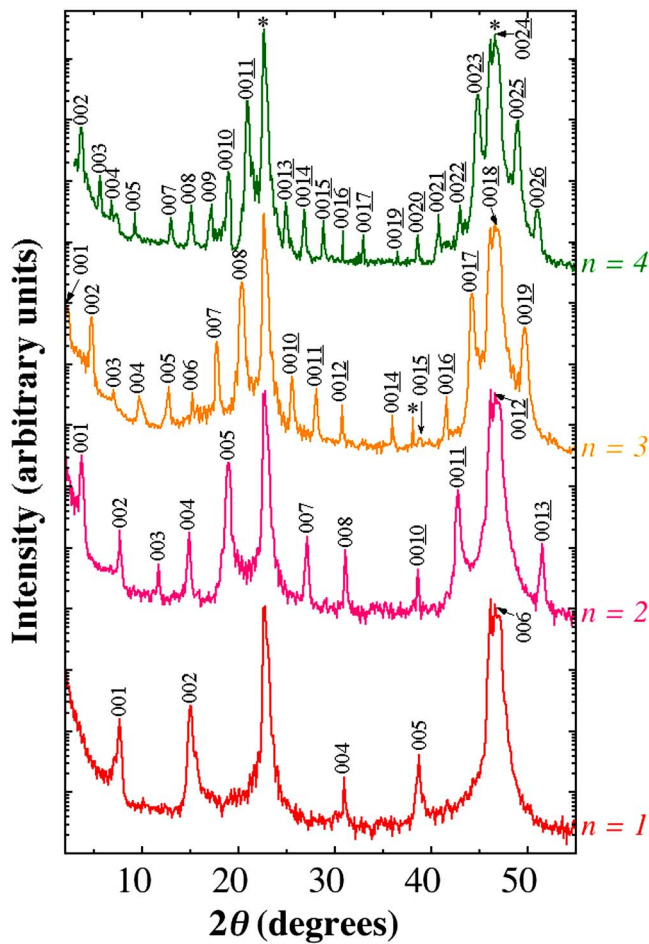
FIG. 1. (Color online) X-ray diffraction θ-2θ patterns of $[(SrMnO_3)_n/(LaMnO_3)_{2n}]_m$ superlattices grown on (100) $SrTiO_3$ with $n=1$, 2, 3, and 4. Substrate peaks are marked with ($*$).

electronic phases depending on the concentration of divalent dopants.[20,21] The interaction between Mn^{3+} and Mn^{4+} ions mediated by oxygen, the so-called double exchange interaction, has been proposed to explain the ferromagnetic order and the metallic behavior for hole-doped manganites.[22] The
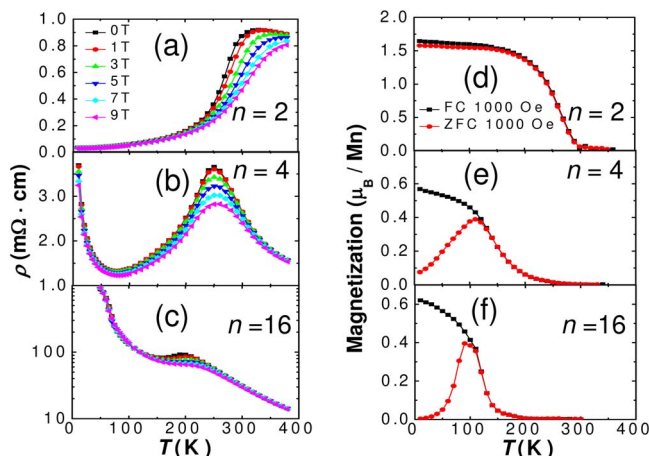
FIG. 2. (Color online) Resistivity as a function of temperature under in-plane applied magnetic fields ranging from 0–9 T, for $[(SrMnO_3)_n/(LaMnO_3)_{2n}]_m$ superlattices with $n=2$ (a), $n=4$ (b), and $n=16$ (c). Corresponding magnetization vs temperature for the superlattices are shown in (d)–(f) for zero-field cooled (ZFC) and field-cooled (FC) conditions in an in-plane magnetic field of 1000 Oe.
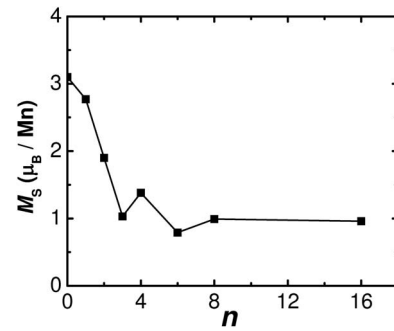
FIG. 3. Saturation magnetization of the superlattices as a function of periodicity, n. $n=0$ represents the $La_{0.67}Sr_{0.33}MnO_3$ solid solution.

valence of the Mn ions in the $SrMnO_3$ layers is 4+, while it is 3+ in the $LaMnO_3$ layers, suggesting that the ferromagnetic metallic behavior in the superlattices with small n could originate from the exchange interaction between Mn^{3+} and Mn^{4+} at the interfaces.[1,4]

Based on the above interpretation, the superlattices should become more resistive and the transition temperature decrease with increase of n because less material is close to the interface between the constituent materials. This is indeed the case, as shown in Figs. 2(b) and 2(c) for $n=4$ and 16, respectively. The superlattice with $n=4$ shows a transition from semiconducting to metallic behavior at 250 K with the resistivity dropping rapidly for temperatures right below the transition temperature, followed by a dramatic increase for temperatures below 90 K. This qualitative behavior is also observed in hole-doped $La_{1-x}Sr_xMnO_3$ for low doping concentrations x and has been attributed to the weak localization of carriers due to disorder.[20] Surprisingly, similar features are still observable for the $n=16$ sample (which consists of a bilayer of $SrMnO_3/LaMnO_3$), as shown in Fig. 2(c), although with much larger resistivity and lower transition temperature.

The temperature dependence of the magnetization of the samples with $n=2$, 4, and 16 is shown in Figs. 2(d)–2(f), respectively. All samples show a sudden increase in magnetization at their apparent ferromagnetic transition temperatures, but the temperature of the apparent magnetic transition is consistently lower than the peak temperature of the resistivity, and much lower in the case of $n=16$. Another surprising feature is the large value of the magnetization and transition temperature for superlattices with larger n ($n=16$), as shown in Fig. 2(f). If one assumes that the exchange interaction happens only at the interface between the $LaMnO_3$ and $SrMnO_3$ layers, one would expect the magnetization to decrease dramatically as n increases and to have a very small value for large n. We find, however, that superlattices with larger n ($n=6$, 8, and 16) still have a fairly large magnetization, that is roughly independent of n, as summarized in Fig. 3. In Fig. 3, the saturation magnetization was obtained by measuring hysteresis loops with an in-plane applied magnetic field up to 4 T.

To explore the source of the large magnetization existing in superlattices with large values of n, we grew a $SrMnO_3/SrTiO_3/LaMnO_3$ trilayer sample with a five unit cell thick $SrTiO_3$ layer in between the $SrMnO_3$ and $LaMnO_3$ layers. The sample configuration of the trilayer is identical to the bilayer with $n=16$, except that it contains the $SrTiO_3$ spacer layer. Surprisingly, the magnetic behavior is quite
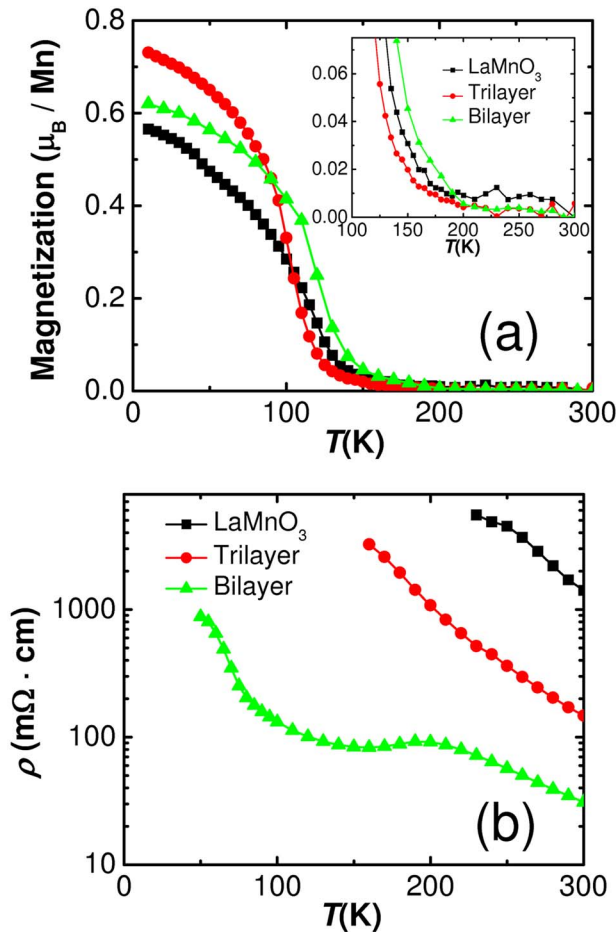
FIG. 4. (Color online) (a) Field-cooled magnetization in an in-plane magnetic field of 1000 Oe and (b) resistivity as a function of temperature for an $LaMnO_3$ thin film, an $n=16$ (bilayer), and an $LaMnO_3/SrTiO_3/SrMnO_3$ (trilayer). Magnetization details are shown in the inset.

similar to that of the superlattice with $n=16$, i.e., similar magnetization and transition temperature. This is unexpected because the magnetic interaction between the $LaMnO_3$ and $SrMnO_3$ layers should have been strongly weakened due to the spacer layer which would result in a much smaller magnetization in the trilayer sample.

In order to clarify this puzzle, we performed magnetic measurements on single-layer $SrMnO_3$ and $LaMnO_3$ films. As expected, $SrMnO_3$ shows no measurable signal. $LaMnO_3$, however, exhibits a large magnetization with a transition temperature of 135 K, as shown in Fig. 4(a). A large magnetization in $LaMnO_3$ thin films has been reported and attributed to the oxygen deficiency in this compound.[23] In our MBE-grown $LaMnO_3$ films, we observe this magnetization to increase with growth or annealing in more oxidizing conditions. This leads us to conclude that excess oxygen, i.e., $LaMnO_{3+\delta}$, is responsible for the large observed magnetization of our $LaMnO_{3+\delta}$ films. Therefore, we attribute the large magnetization observed in the trilayer and the superlattices with large n to mainly the $LaMnO_3$ constituent layers, with a small proportion of the total magnetization introduced from the interface due to the magnetic interaction between Mn^{3+} and Mn^{4+}. Although there might be a magnetization contribution from the $LaMnO_3$ layers of the superlattices with smaller n, the interface magnetism is significant and accounts

for the resulting large magnetizations and high transition temperatures of the superlattices with low n.

In contrast to the magnetization, the electronic transport of the samples is dominated by the effects of the interfaces, as shown in Fig. 4(b). While the $n=16$ bilayer has electronic transport which manifests the onset of ferromagnetism through the previously mentioned peak in $\rho(T)$, the trilayer and the pure $LaMnO_3$ film have much higher resistivities. This indicates that exchange across the interface is still leading to local ferromagnetism, even in the case where there is only a single interface. Subtracting out the background saturation magnetization of the $LaMnO_3$ (about $1\mu_B/Mn$) from Fig. 3 indicates that the charge exchange at the $SrMnO_3/LaMnO_3$ interface falls of over a distance of about 1 nm, which is consistent with theoretical predictions.[24] This finding has implications for the engineering of epitaxial heterostructures which take advantage of the charge exchange at the interface and the resultant local properties.

[1]P. A. Salvador, A.-M. Haghiri-Gosnet, B. Mercey, M. Hervieu, and B. Raveau, Appl. Phys. Lett. **75**, 2638 (1999).

[2]I. Panagiotopoulos, C. Christides, N. Moutis, M. Pissas, and D. Niarchos, J. Appl. Phys. **85**, 4913 (1999).

[3]K. S. Takahashi, M. Kawasaki, and Y. Tokura, Appl. Phys. Lett. **79**, 1324 (2001).

[4]T. Koida, M. Lippmaa, T. Fukumura, K. Itaka, Y. Matsumoto, M. Kawasaki, and H. Koinuma, Phys. Rev. B **66**, 144418 (2002).

[5]A. Ohtomo and H. Y. Hwang, Nature (London) **427**, 423 (2004).

[6]P. Murugavel, P. Padhan, and W. Prellier, Appl. Phys. Lett. **85**, 4992 (2004).

[7]X. Ke, M. S. Rzchowski, L. J. Belenky, and C. B. Eom, Appl. Phys. Lett. **84**, 5458 (2004).

[8]H. Yamada, M. Kawasaki, T. Lottermoser, T. Arima, and Y. Tokura, Appl. Phys. Lett. **89**, 052506 (2006).

[9]S. Thiel, G. Hammerl, A. Schmehl, C. W. Schneider, and J. Mannhart, Science **313**, 1942 (2006).

[10]A. Brinkman, M. Huijben, M. van Zalk, J. Huijben, U. Zeitler, J. C. Maan, W. G. van der Wiel, G. Rijnders, D. H. A. Blank, and H. Hilgenkamp, Nat. Mater. **6**, 493 (2007).

[11]N. Reyren, S. Thiel, A. D. Caviglia, L. Fitting Kourkoutis, G. Hammer, C. Richter, C. W. Schneider, T. Kopp, A.-S. Ruetschi, D. Jaccard, M. Gabay, D. A. Muller, J.-M. Triscone, and J. Mannhart, Science **317**, 1196 (2007).

[12]A. Bhattacharya, X. Zhai, M. Warusawithana, J. N. Eckstein, and S. D. Bader, Appl. Phys. Lett. **90**, 222503 (2007).

[13]S. J. May, S. G. E. te Velthuis, M. R. Fitzsimmons, X. Zhai, J. N. Eckstein, S. D. Bader, and A. Bhattacharya, e-print arXiv:cond-mat/0709.1715.

[14]A. Bhattacharya, S. J. May, S. G. E. te Velthuis, M. Warusawithana, X. Zhai, A. B. Shah, J.-M. Zuo, M. R. Fitzsimmons, S. D. Bader, and J. N. Eckstein, e-print arXiv:cond-mat/0710.1452.

[15]F. Moussa, M. Hennion, J. Rodriguez-Carvajal, H. Moudden, L. Pinsard, and A. Revcolevschi, Phys. Rev. B **54**, 15149 (1996).

[16]T. Takeda and S. Ōhara, J. Phys. Soc. Jpn. **37**, 275 (1974).

[17]J. H. Haeni, C. D. Theis, and D. G. Schlom, J. Electroceram. **4**, 385 (2000).

[18]G. Koster, B. L. Kropman, G. J. H. M. Rijnders, D. H. A. Blank, and H. Rogalla, Appl. Phys. Lett. **73**, 2920 (1998).

[19]J. B. Nelson and D. P. Riley, Proc. Phys. Soc. London **57**, 160 (1945).

[20]A. Urushibara, Y. Moritomo, T. Arima, A. Asamitsu, G. Kido, and Y. Tokura, Phys. Rev. B **51**, 14103 (1995).

[21]P. Schiffer, A. P. Ramirez, W. Bao, and S.-W. Cheong, Phys. Rev. Lett. **151**, 3336 (1995).

[22]C. Zener, Phys. Rev. **81**, 440 (1951).

[23]A. Gupta, T. R. McGuire, P. R. Duncombe, M. Rupp, J. Z. Sun, W. J. Gallagher, and G. Xiao, Appl. Phys. Lett. **67**, 3494 (1995).

[24]I. Gonzalez, S. Okamoto, S. Yunoki, A. Moreo, and E. Dagotto, J. Phys. Cond. Mat. (to be published).